

1 **Assessing the risk of climate maladaptation for Canadian polar bears**

2

3 L. Ruth Rivkin^{1,2,3,†}, Evan S. Richardson⁴, Joshua M. Miller^{2,3,5}, Todd C. Atwood⁶, Steven
4 Baryluk⁷, Erik W. Born⁸, Corey Davis⁹, Markus Dyck^{10,*}, Evelien de Greef¹, Kristin L. Laidre¹¹,
5 Nicholas J. Lunn¹², Sara McCarthy¹³, Martyn E. Obbard^{14,15}, Megan A. Owen³, Nicholas W.
6 Pilfold³, Amelie Roberto-Charron¹⁰, Øystein Wiig¹⁶, Aryn P. Wilder³, Colin J. Garroway¹

7

8 **Author Affiliations**

9 ¹ Department of Biological Sciences, University of Manitoba, Winnipeg, Manitoba, Canada.

10 ² Polar Bears International, Bozeman, Montana, United States of America, USA.

11 ³ San Diego Zoo Wildlife Alliance, Escondido, California, USA.

12 ⁴ Wildlife Research Division, Science and Technology Branch, Environment and Climate Change
13 Canada, Winnipeg, Manitoba, Canada.

14 ⁵ MacEwan University, Edmonton, Alberta, Canada.

15 ⁶ U.S. Geological Survey, Alaska Science Center, Anchorage, Alaska, USA.

16 ⁷ Department of Environment and Climate Change, Government of the Northwest Territories,
17 Inuvik, Northwest Territories, Canada.

18 ⁸ Greenland Institute of Natural Resources, Nuuk, Greenland

19 ⁹ Department of Biological Sciences, University of Alberta, Edmonton, Alberta, Canada; ORCID
20 0000-0003-4362-0659

21 ¹⁰ Department of Environment, Government of Nunavut, Igloolik, Nunavut, Canada.

22 ¹¹ Polar Science Center, Applied Physics Laboratory, University of Washington, Seattle WA USA

23 ¹² Wildlife Research Division, Science and Technology Branch, Environment and Climate
24 Change Canada, Edmonton, Alberta, Canada.

25 ¹³ Wildlife Division, Department of Fisheries, Forestry and Agriculture; Government of
26 Newfoundland and Labrador, Happy Valley-Goose Bay, Newfoundland and Labrador, Canada.

27 ¹⁴ Wildlife Research and Development Section, Ontario Ministry of Natural Resources, Trent
28 University, Peterborough, Ontario, Canada. ORCID 0000-0003-2064-0155.

29 ¹⁵ Environmental and Life Sciences Graduate Program, Trent University, Peterborough, Ontario,
30 Canada

31 ¹⁶ Natural History Museum, University of Oslo, Oslo, Norway

32

33 † Corresponding author: Ruth Rivkin, Department of Biological Sciences, University of
34 Manitoba, 66 Chancellors Cir, Winnipeg, MB R3T 2N2, Canada. ruthrivkin@gmail.com

35 * Deceased

36

37 **Running Head:** Genetic vulnerability of polar bears

38 **Article Type:** Letter

39 **Keywords:** Adaptation, gene flow, genetic offset, genetic variation, sea ice loss, polar bear,

40 *Ursus maritimus*

41 **Word Count:** Abstract (150); Main text (4,963); References (85); Tables (1); Figures (3)

42 **Availability of Data and Code**

43 Genotype files and code will be archived upon acceptance for publication.

44

45 **Author Contributions**

46 Conceptualization: LRR, CJG, ESR

47 Data curation: LRR, JMM

- 48 Formal analysis: LRR, ED
- 49 Investigation: LRR
- 50 Writing - original draft preparation: LRR
- 51 Writing - review and editing: All authors
- 52 Funding acquisition: LRR; ESR; CJG
- 53 Resources and samples: ØW, KLL, MD, MEO, ESR, NL, SB, EWB, SM, TCA, AR-C

54 **Abstract**

55 The Arctic is warming four times faster than the rest of the world, threatening the persistence
56 of Arctic species. It is uncertain if Arctic wildlife will have sufficient time to adapt to such
57 rapidly warming environments. We used genetic forecasting to measure the risk of maladaptation
58 to warming temperatures and sea ice loss in polar bears (*Ursus maritimus*) sampled across the
59 Canadian Arctic. We found evidence for local adaptation to sea ice condition and
60 temperature. Forecasting of genome-environment mismatches for predicted climate scenarios
61 suggested that polar bears in the high Arctic had the greatest risk of becoming maladapted to
62 climate warming. While bears in the high Canadian Arctic may be most likely to become
63 maladapted, all polar bears face potentially negative outcomes to climate change. Given the
64 importance of the sea ice habitat to polar bears, we expect that the increased risk of
65 maladaptation to future warming is already widespread.

66

67

68 **Introduction**

69 Climate change is a major contributor to the biodiversity crisis, with many species threatened
70 with extinction due to habitat loss (IPCC 2023). The vulnerability of species to climate change is
71 determined by multiple interacting factors, including population size, dispersal capabilities,
72 genetic background, and adaptive capacity (Thomas et al. 2004; Pacifici et al. 2015). Adaptive
73 capacity can help species cope with climate change; however, the pace of environmental change
74 may prove to be too rapid for some species to adapt (Berteaux et al. 2004). Spatial variation in
75 environments adds an additional layer of complexity to species responses to climate change.
76 Identifying the spatial and environmental drivers of local adaptation supports assessments of a
77 species' potential for maladaptation to future environments under climate change.

78 The Arctic is warming at 2-4x the global average (Cohen et al. 2014; Previdi et al. 2021;
79 Rantanen et al. 2022). Increased temperatures have led to significant changes in sea ice
80 conditions. Annual sea ice forms later and melts earlier in the year compared to previous
81 decades, creating sea ice with reduced thickness and less spatial coverage (Comiso et al. 2008;
82 Screen and Simmonds 2010; Stroeve et al. 2014; Kwok 2018; Laidre et al. 2018). Even under
83 moderate emission scenarios, the Arctic could become ice-free in the summer as early as the
84 mid-2030s (Docquier and Koenig 2021; Kim et al. 2023; Shen et al. 2023). The high Arctic
85 (>68 °N) is predicted to experience some of the largest environmental changes associated with
86 climate change, as warming temperatures have reduced the extent of multiyear sea ice (i.e., ice
87 that has survived at least two years of summer melt) by more than 90% (Kwok 2018; Stroeve
88 and Notz 2018). The loss of sea ice has significant implications for the Arctic ecosystem,
89 particularly for species that depend on sea ice for survival.

90 Climate-mediated reductions in the extent of sea ice habitat represents the single greatest
91 threat to the persistence of Arctic species (Amstrup et al. 2008; Marcot et al. 2023). Polar bears
92 (*Ursus maritimus*) are ice-adapted predators that rely on sea ice for hunting, migration, and
93 mating (Regehr et al. 2016; Stern and Laidre 2016). Polar bears forage intensively on sea ice,
94 hunting ringed (*Pusa hispida*) and bearded seals (*Erignathus barbatus*) as their primary food
95 source (Stirling and Archibald 1977; Wiig et al. 2008). Sea ice loss due to climate warming
96 influences habitat use and connectivity among polar bears (Durner et al. 2009; Laidre et al. 2018).
97 When seasonal sea ice melts in southern regions of the Arctic, polar bears are restricted to land
98 and typically fast until the sea ice returns. Accelerating sea ice loss increases the time polar bears
99 spend on land (Rode et al. 2015; Atwood et al. 2016; Lunn et al. 2016; Laidre et al. 2018),
100 elevating their exposure to disease pathogens (Pilfold et al. 2021) and anthropogenic food
101 sources (Smith et al. 2023; Stimmelmayer et al. 2023), and exacerbating human-bear conflict
102 (Wilder et al. 2017; Heemskerk et al. 2020). Extended fasting periods lead to declines in body
103 condition, reproductive output, and survival of polar bears (Regehr et al. 2007; Stirling and
104 Derocher 2012; Lunn et al. 2016). As the ice-free period continues to increase, polar bears may
105 face local extirpation as they are pushed beyond their physiological fasting limits (Molnár et al.
106 2020).

107 Despite extensive knowledge of the effects of sea ice loss on polar bear ecology, there are
108 relatively few studies on the evolutionary responses of polar bears to climate change. Modern
109 polar bears have lower levels of genetic diversity than their nearest relatives, grizzly bears
110 (Miller et al. 2012; Liu et al. 2014, Lan et al. 2022). Some polar bears have experienced
111 additional genetic diversity losses and increased genetic isolation associated with recent sea ice
112 loss (Maduna et al. 2021). These findings suggest that changes in ice availability may alter

113 patterns of gene flow and genetic drift (Laidre et al. 2022), potentially limiting the ability of
114 polar bears to adapt to climate change. However, the adaptive capacity of polar bears to warming
115 climates in the Arctic remains unknown.

116 Genetic forecasting is a tool that can be used to inform predictions of whether polar bears
117 can adapt to a warming Arctic. These predictive models can be used to assess if mismatches exist
118 between current population allele frequencies and the future environments those populations are
119 likely to experience (Capblancq et al. 2020). Populations with a higher degree of mismatch
120 (genetic offsets *sensu* Fitzpatrick and Keller 2015) are at risk of maladaptation to climate change,
121 particularly if they are genetically isolated or have low fitness (Láruson et al. 2022). Quantifying
122 genetic offsets at the population level allows us to assess potential vulnerability to climate
123 change across polar bear management-designated populations, known as subpopulations.

124 We assessed the risk of maladaptation to climate change in polar bears across the
125 Canadian Arctic. We asked 1) how does standing genetic variation and population structure vary
126 among subpopulations?; 2) do sea ice loss and warming air temperatures affect allele turnover in
127 polar bears?; and 3) are genetic offsets to future environments variable among subpopulations?
128 We predicted that polar bear subpopulations that face the greatest amount of environmental
129 change (i.e., those in the high Arctic) will have the greatest genetic offsets to future
130 environments, leading to an increased risk of maladaptation.

131

132 **Materials and methods**

133 **Study system and genotype processing**

134 Polar bears are distributed across the Arctic in 19 subpopulations recognized by the International
135 Union for the Conservation of Nature (IUCN; Obbard et al. 2010). Subpopulation boundaries

136 were determined by satellite telemetry data, ecological and genetic differences among bears, and
137 regional differences in management policy (Obbard et al. 2010). There are 14 polar bear
138 subpopulations within Canada's borders (Figure 1A), some of which are shared with Greenland
139 and the USA. These subpopulations range in abundance from 160-2800 individuals (Table 1;
140 IUCN/SSC 2021). We categorized the Canadian subpopulations included in our study as high
141 Arctic (>68 °N), low Arctic (55-68 °N), and sub-Arctic (<55 °N) following the Arctic
142 Biodiversity Assessment Arctic Zones guideline (Table 1; Meltotte et al., 2013).

143 Two single nucleotide polymorphism (SNP) arrays have been developed for polar bears
144 and used to assess population structure, heritability, and hybridization (Malenfant et al. 2015,
145 2018; Miller et al. in review at Conservation Genetic Resources, included in supporting
146 information). A total of 1,450 polar bears were genotyped on the *Ursus maritimus* V1 SNP chip,
147 a 9K Illumina Infinium Bead Chip containing a combination of transcriptome-derived and RAD-
148 derived SNPs (Malenfant et al. 2015). Bears genotyped on the *Ursus maritimus* V1 SNP chip
149 primarily originated from the Hudson Bay and were sampled between 1985-2012. Another 628
150 polar bears were genotyped on the *Ursus maritimus* V2 SNP chip, an 8K Illumina Infinium Bead
151 Chip containing loci from the V1 SNP chip augmented to include species diagnostic loci (Miller
152 et al. in review). Bears genotyped on this chip originated from the circumpolar Arctic and were
153 sampled between 1975-2015. Additional sampling and harvesting details can be found in
154 Malenfant et al. (2015) and Miller et al. (in review). Bears that were genotyped on both chips
155 have a 99% genotyping concordance (Miller et al. in review), and thus we are confident in the
156 genotypes of individuals from both chips.

157 We used the genotype files generated by Miller et al. (in review) for our analyses. We
158 selected SNPs present on both SNP chips ($N = 4,723$ SNPs) and removed individuals that were

159 not georeferenced. To avoid uneven sample sizes and improve the performance and speed of the
160 genetic offset models, we selected a maximum of 50 bears per subpopulation. For
161 subpopulations which contained more than 50 sampled bears, we preferentially selected bears
162 with a complete set of environmental data points and with no missing genotype calls. We also
163 removed the single individual that was sampled from the Arctic Basin subpopulation. We quality
164 filtered on our final sample set using PLINK v1.90 (Chang et al. 2015) to remove SNPs with a
165 genotyping rate below 90% (*--geno 0.1*), a minor allele frequency below 1% (*--maf 0.01*), and
166 that were in linkage disequilibrium (*--indep-pairwise 10 1 0.1*). For the genetic diversity and
167 differentiation analyses, we also removed SNPs that were out of Hardy-Weinberg equilibrium
168 (HWE; *--hwe 0.001 midp*).

169 **Genetic diversity and differentiation**

170 We assessed standing genetic variation and differentiation among polar bear subpopulations. We
171 used the *--het* call in PLINK to calculate individual per-locus level estimates of observed
172 heterozygosity (H_o), and inbreeding (F), then averaged values across subpopulations. We used
173 the *pi* function from the R v4.3.0 (R Core Team 2023) package radiator v1.2.8 (Gosselin et al.
174 2020) to calculate nucleotide diversity (π) for each subpopulation (Nei and Li 1979). The
175 transcriptomic loci on the SNP chips were ascertained using the Western Hudson Bay (WH)
176 subpopulation which can inflate estimates of genetic diversity for WH relative to other
177 subpopulations. To account for this inflation, we repeated the calculations of H_o and π on the
178 transcriptomic-derived ($N = 1,381$ SNPs) and RAD-derived loci ($N = 2,304$ SNPs) separately.

179 We calculated pairwise F_{ST} among subpopulations using the *stamppFst* function in the
180 StaMMP v1.6.3 R package (Pembleton et al. 2013). We bootstrapped across loci 100 times to
181 generate 95% confidence intervals for each pairwise F_{ST} value to determine if subpopulations

182 were significantly differentiated from one another. Lastly, we calculated the number of private
183 alleles per subpopulation using the *gl.report.pa* function from the R package dartR v2.9.5
184 (Gruber et al. 2018).

185 **Population structure analyses**

186 Given that polar bears have been grouped into subpopulations for management purposes, we
187 were interested in determining if the genetic structure of individuals corresponded to their
188 subpopulation designation. We used two complementary methods to assess population structure.
189 First, we estimated individual ancestry coefficients using sparse non-negative matrix
190 factorization (sNMF; Frichot et al. 2014), implemented with the *snmf* function from the R
191 package LEA v3.12.2 (Frichot and François 2015). sNMF takes an unsupervised approach to
192 estimate individual admixture coefficients from multilocus genotype data comparable to those
193 from STRUCTURE and ADMIXTURE (Frichot et al. 2014). We identified the optimal number
194 of clusters by comparing the fit of each model with $K = 1-13$ clusters. We ran each model 10
195 times and selected the value of K with the lowest cross-entropy score. We generated admixture
196 plots to visualize how individuals formed clusters, and then mapped the results on to each
197 subpopulation location. Lastly, we extracted the cluster assignment for each bear for later use in
198 the genetic offset analysis. We assigned an individual to a cluster if it had an ancestry proportion
199 greater than 0.75 to any single cluster. If ancestry to any cluster was lower than 0.75, the
200 individual was assigned as admixed.

201 We conducted a spatial principal component analysis (sPCA) to identify spatial patterns in
202 genetic variation among individuals. sPCA uses an ordination-based approach to maximize the
203 variation between allele frequency and spatial autocorrelation estimated with Moran's I (Jombart
204 and Ahmed 2011). The eigenvectors generated by the sPCA are mapped onto geographic

205 coordinates, allowing for clines in genetic structure to be evaluated (Jombart and Ahmed 2011).
206 We used the function *chooseCN* from the *adegenet* v2.1.10 package (Jombart and Ahmed 2011)
207 to create a Delauney's triangulation connection network and account for continuously distributed
208 individuals across the range (Jombart et al. 2008). We first ran a sPCA model that included all
209 axes using the *spca* function from *adegenet*. We ran permutation tests with 999 permutations to
210 identify if a significant effect of global structure existed in the data. We retained the first five
211 positive (global) eigenvalues which contributed most strongly to variance in the final model. We
212 visualized genetic similarity among individuals using the *colorplot* function from *adegenet* to
213 plot the lagged principal component (PC) scores on a map.

214 **Environmental variable selection**

215 We quantified present and future conditions for sea ice and air temperature across the Canadian
216 Arctic. We extracted mean annual ice thickness (m) and ice cover (%) from the Bio-ORACLE
217 v2.0 database (Assis et al. 2018). Annual sea ice thickness is a measure of how thick the ice is at
218 a given sampling area averaged across the year, whereas annual sea ice cover is a measure of
219 how much of the sampling area is covered by ice throughout the year. Bio-ORACLE marine
220 layers are available as monthly and annual averages for present conditions (2000–2014) at a
221 spatial scale of 9.2 km at the equator (5 arcmin; Assis et al. 2018). We used the R package
222 *sdmpredictors* v0.2.14 (Bosch and Fernandez 2021) to extract values at each sampling location
223 with a 50 km² buffer surrounding each site to account for bear movement. We also extracted ice
224 thickness values from future (2040-2050 and 2090-2100) conditions that were forecasted under
225 RCP8.5 (IPCC 2014). Forecasted ice thickness was sourced from three coupled Atmosphere–
226 Ocean General Circulation Models (AOGCM) provided by Coupled Model Intercomparison
227 Project Phase 5 (CMIP5; Assis et al. 2018). We selected RCP8.5 because this level of climate

228 warming is predicted to occur if no mitigation practices are put into place (Brown et al. 2020).
229 Ice concentration has not yet been included in the future climate scenarios dataset in Bio-
230 ORACLE, so we did not include this predictor in our future environment dataset.

231 We followed a similar approach to extract near-surface air temperature averaged from
232 2000-2014 from each sampling location. We used the StableClim database (Brown et al. 2020) to
233 extract mean annual temperature surrounding 50 km² from each sampling location. Air
234 temperature under RCP8.5 was sourced from all 19 AOCMs from CMIP5 (Brown et al. 2020).
235 StableClim has at a spatial scale of 278 km at the equator (150 arcmin, so we used the R package
236 raster v3.6-20 (Hijmans 2023) to match the extent of the temperature layer to the ice condition
237 layers. We extracted values under the same timelines (present and future) and climate scenario as
238 the ice condition layers.

239 **Gradient Forest predictions of maladaptation**

240 We assessed the risk of genetic maladaptation to climate warming using Gradient Forests (GF), a
241 nonparametric machine learning approach that can be used to assess changes in allele
242 frequencies across environmental and spatial gradients (Fitzpatrick and Keller 2015). GF builds
243 regression trees using Random Forests (Breiman 2001) and creates turnover functions that
244 determine how well environmental change along the gradients explains changes in individual
245 allele frequencies. A goodness-of-fit measure (R^2) is generated from each regression tree and
246 used to weight predictors in proportion to their accuracy and importance in explaining allele
247 turnover (Ellis et al. 2012). Importantly, the relative importance of predictors on allele turnover
248 can be interpreted even when R^2 are small.

249 Turnover functions can be aggregated across alleles to generate a cumulative importance
250 curve for the entire genome (Láruson et al. 2022). The slope of the importance curve describes

251 the rate of change in allele frequency across the environmental gradient; steeper curves indicate
252 greater allele turnover. The underlying assumption of this method is that populations are locally
253 adapted to their current environment; any shift in allele frequency along the environmental
254 gradient is presumed to be maladaptive. Maladaptation can be quantified with genetic offset
255 scores, which are the Euclidean distance between current and future allele frequencies under
256 current and future environmental gradients (Ellis et al. 2012). The greater the distance, the
257 greater the mismatch between current allele frequencies and future environments, and the greater
258 the risk of maladaptation.

259 We implemented the GF with the gradientForest v0.1-34 package in R (Smith and Ellis
260 2013) using the sea ice and air temperature as environmental predictors. We ran separate models
261 for sea ice thickness and cover because these variables were highly correlated ($r = 0.82$). Both
262 models included temperature as a co-factor. We imputed missing SNPs with the *impute* function
263 from the LEA package using the most likely genotype value computed from the genotype matrix.
264 To account for spatial variation in population abundances and genetic structure, including
265 isolation-by-distance (IBD), we included a matrix of uncorrelated spatial variables in the models
266 (Láruson et al. 2022). We calculated distance-based Moran's eigenvector maps (PCNMs) with
267 the *pcnm* function in the R package *vegan* v2.6-4 (Oksanen 2015). We retained the first half of
268 the positive PCNMs ($N = 62$) in the model, which represent broad-scale spatial autocorrelation
269 patterns (Fitzpatrick and Keller 2015). We set the number of trees to 500 (*ntree* = 500) with 201
270 bins to compact splits (*nbin* = 201) and a predictor correlation threshold above 0.5
271 (*corr.threshold* = 0.5). We assigned the maximum number of splits using the default settings for
272 gradientForest (Smith and Ellis 2013). We visualized the environmental change in our study area
273 with PCA biplots and mapped the compositional distribution of alleles across the area.

274 We used the GF model output to calculate genetic offset scores for each polar bear under
275 ice thickness and temperature conditions in 2050 and 2100. We created raster maps of the offset
276 score for each pixel, then extracted offset score for each sampling location. We ran a generalized
277 linear model with a quasi-binomial distribution to test for differences in individual genetic offsets
278 among polar bears. We included location in the Arctic (high, low, and sub-Arctic), genetic cluster
279 (Clusters 1-5, or admixed), subpopulation abundance, and climate projection year (2050 or 2100)
280 as predictor variables. We assessed the assumptions of the model by plotting residuals and
281 examining collinearity between predictors. We tested the significance of predictors using the
282 *anova.glm* function from the R stats v4.3.0 package (R Core Team 2023).

283

284 **Results**

285 **Population genetic diversity**

286 The HWE-filtered dataset contained 3,685 SNPs from 411 bears sampled from 13
287 subpopulations in Canada between 1985-2016. Subpopulations contained an average of 32
288 individuals (range: 10-50; Table 1). Across all SNPs, mean H_O was 0.263 and mean F was 0.037
289 (Table 1, Figure S1). Norwegian Bay (NW) had the lowest heterozygosity and highest inbreeding
290 values ($H_O = 0.240$, $F = 0.121$), whereas Kane Basin (KB) had the highest heterozygosity and
291 lowest inbreeding values ($H_O = 0.271$, $F = 0.017$). Nucleotide diversity for the entire population
292 was 0.137 (Table 1). As with H_O , nucleotide diversity was lowest in NW ($\pi = 0.118$) but was
293 greatest ($\pi = 0.133$) in Foxe Basin (FB), Davis Straight (DS), and Western Hudson Bay (WH).
294 Genetic diversity was ~50% higher in transcriptomic-derived SNPs relative to RAD-derived
295 SNPs as expected (Table S1) but was lowest in NW for both sets of SNPs, consistent with
296 observations from the HWE-filtered dataset.

297 Global F_{ST} was 0.035. Pairwise F_{ST} ranged from 0.001 to 0.089 (Table S2) and were
298 significantly differentiated from one another ($p < 0.05$) except for Kane Basin and Baffin Bay (p
299 = 0.29). Lastly, we identified a mean of 420 private alleles per subpopulation (Table 1), with the
300 greatest number being found in NW ($N = 747$ alleles).

301 **Population genetic structure**

302 We identified $K = 5$ genetic clusters of polar bears as the best fitting model with a cross-entropy
303 score of 0.648 (range 0.671-0.648; Figure S2). The Norwegian Bay (NW) subpopulation formed
304 a unique genetic cluster (Cluster 3; Figure 1). The Hudson Bay subpopulations formed a single
305 cluster (Cluster 5), which included Western Hudson Bay (WH), Southern Hudson Bay (SH), and
306 Foxe Basin (FB), as did the Southern and Northern Beaufort Sea (SB and NB, respectively)
307 subpopulations (Cluster 4). Viscount Melville Sound (VM) and M'Clintock Channel (MC)
308 formed a cluster (Cluster 1), while the remaining subpopulations shared ancestry (Cluster 2) with
309 some degree of admixture.

310 Polar bears were most likely to share genetic variation with those in closest proximity to
311 them, suggesting that IBD contributes to genetic structure across the Canadian Arctic. The
312 permutation test from the sPCA analysis identified a significant effect of global structure (p -
313 value < 0.01), indicating that genetic structure is best explained by the positive spatial
314 autocorrelation among individuals. Visualization of the lagged PC scores confirmed patterns of
315 IBD, where genetic similarity gradually declined with distance (Figure S3).

316 **Gradient Forest model of allele turnover**

317 Ice thickness and near surface air temperature were among the top five most important predictors
318 of allele turnover ($N = 3,830$ linkage-pruned SNPs) across all samples. Mean weighted R^2 of the
319 GF model was 0.0018. The top ranked predictor variables were two spatial variables that

320 accounted for turnover in alleles associated with latitude, population abundance, and genetic
321 structure (PCNM-2: $R^2 = 0.014$; PCNM4: $R^2 = 0.008$; Figure S4). Ice thickness was the third
322 ranked predictor ($R^2 = 0.008$). The largest turnovers in allele frequency along the ice thickness
323 gradient occurred between 2-3 m of ice depth (Figure 2a). Temperature was the fifth ranked
324 predictor ($R^2 = 0.004$), with the largest turnover in alleles occurring at $-5\text{ }^\circ\text{C}$ (Figure 2a). We
325 found similar results for the model with ice cover and temperature, with the largest turnover in
326 alleles occurring at 60% ice cover (Fig. S5; Supplementary Results).

327 PC scores generated from the environmental variables mapped into geographic space
328 demonstrate a split in genetic composition between high Arctic polar bears and the rest of the
329 population (Figure 2b). The PCA biplot indicates that ice thickness and temperature were
330 uncorrelated but had similar loading magnitudes, suggesting that while they both contribute to
331 the genetic similarity among bears, the predictors explain different components of the variation
332 (Figure 2b inset). Changes in ice thickness explained variation between the Beaufort Sea and the
333 rest of the bears, whereas changes in temperature contributed to variation across the entire
334 sampled range.

335 **Genetic offsets**

336 Genetic offsets were predicted to be highest in the high Canadian Arctic (Figures 3 and S6). We
337 found that offset scores differed between location ($F_{2,796} = 64.01$, $p < 0.001$), genetic cluster
338 ($F_{5,796} = 20.11$, $p < 0.001$), and abundance ($F_{1,796} = 33.17$, $p < 0.001$). Offset scores were greatest
339 in bears in the high Arctic (Figure 3a, c), particularly Viscount Melville Sound (VM) and
340 Norwegian Bay (NW). Polar bears from the Hudson Bay and Davis Strait (DS) had the lowest
341 offset scores. Genetic offsets declined as subpopulation abundance increased ($b = -1.96 \times 10^{-4}$,
342 Figure 3b). Offset scores were greater under the climate projections for 2100 compared to 2050

343 ($F_{1,796} = 74.74$, $p < 0.001$), but the effect of location and population size remained consistent
344 between projection years.

345

346 **Discussion**

347 We examined genetic offset scores under projected climate warming to assess the potential for
348 maladaptation to climate change in polar bears in Canada. We identified turnover in allele
349 frequencies that corresponded to changes in sea ice and temperature gradients. Polar bear
350 subpopulations in the Canadian high Arctic and those with low population abundances had the
351 highest genetic offset scores, suggesting that these subpopulations may be the most vulnerable to
352 climate change. We also found that the Norwegian Bay (NW) subpopulation in the high Arctic
353 had the lowest levels of standing genetic variation and was genetically isolated from other
354 subpopulations. Our findings can help inform science-based conservation and harvesting
355 strategies with the capacity to target specific subpopulations (Peacock et al. 2011) and shed light
356 on the difficulties ice-adapted Arctic species will have in response to climate warming.

357 We identified points along the ice and temperature gradients associated with large turnover
358 in allele frequencies. Allele frequency turnover peaked at approximately 2 m of ice thickness,
359 60% ice cover, and at $-5\text{ }^{\circ}\text{C}$. Allele turnover points at 2 m thickness are consistent with those
360 found in the high Arctic, whereas 60% ice cover and $-5\text{ }^{\circ}\text{C}$ temperatures occur more frequently in
361 the low and sub-Arctic. Ice condition was the strongest environmental driver of allelic turnover,
362 likely reflecting differences in regions of the Arctic with thick multiyear sea ice versus thin
363 seasonal sea ice. Consequently, our analysis may be capturing different aspects of local
364 adaptation between low/sub-Arctic subpopulations and high Arctic subpopulations. Ice thickness

365 may be a more influential predictor for high Arctic polar bears that are experiencing rapid
366 thinning of multiyear ice compared to bears farther south (Stroeve and Notz 2018).

367 The reliance on multiyear sea ice may explain why we observed greater genetic offsets in
368 the high Arctic. Declines in ice thickness likely contribute to allelic mismatch in some high
369 Arctic subpopulations, such as Viscount Melville Sound (VM) and Norwegian Bay (NW), which
370 had the highest offset scores. However, decreasing sea ice thickness may provide temporary
371 benefits to some subpopulations due to increased marine productivity in areas that were
372 previously covered by multiyear sea ice (Yool et al. 2015). Between 1990 and 2010, Kane Basin
373 (KB) transitioned from a multiyear ice habitat to a seasonal ice habitat (Laidre et al. 2020). Polar
374 bears in KB have shown improvements in body condition and increased range sizes, suggesting
375 that they are benefitting from sea ice loss (Laidre et al. 2020). We found that KB had higher
376 genetic diversity than many other subpopulations, but also had high offset scores, suggesting that
377 continued sea ice loss may become problematic for the subpopulation. Interestingly, Southern
378 Hudson Bay (SH), the only sub-Arctic subpopulation, had the lowest genetic offsets and
379 increased in abundance between 2016-2021 (Northrup et al. 2021), potentially indicating some
380 degree of robustness to climate change.

381 Variation in genetic offset scores across the Arctic suggests that subpopulations differ in
382 their potential for adaptation to climate change (Fitzpatrick et al. 2021). Adaptation depends on
383 the strength of selection imposed by the environment, standing genetic variation within each
384 population, and the rate of gene flow between populations. The efficacy of selection is weaker in
385 small populations and when standing genetic variation is reduced (Barrett and Schluter 2008;
386 Charlesworth 2009). We found that genetic offset scores were negatively correlated with
387 subpopulation abundance, consistent with the hypothesis that small population sizes reduce

388 adaptive capacity (Charlesworth 2009). This trend was observed even after accounting for spatial
389 variation in population abundance with the PCNMs. We also identified the lowest genetic
390 diversity in NW, which combined with its small abundance, suggests that NW may have less
391 capacity to adapt to climate warming than other subpopulations.

392 We identified two spatial predictors as the most influential drivers of allele turnover. These
393 predictors corresponded to variation in latitude and population abundance and suggest the
394 presence of IBD among polar bears. If bears from the southern Arctic migrate north, they may
395 introduce alleles adapted to warmer conditions into high Arctic subpopulations. For example, a
396 small, isolated population of polar bears in southeastern Greenland that relies on glacial ice
397 rather than sea ice may could serve as a critical source of adaptive alleles for populations farther
398 north (Laidre et al. 2022). Although polar bears are capable of long-distance dispersal (Durner
399 and Amstrup 1995), the effects of climate change on dispersal rate are variable (Ferguson et al.
400 2002; Pagano et al. 2021). Our sPCA identified evidence of IBD among polar bears, suggesting
401 that while dispersal does occur, it is limited by the distance. Consequently, the rate of gene flow
402 may be insufficient to prevent maladaptation of Canadian high Arctic polar bears.

403 In addition to patterns of IBD, we identified five genetic clusters of polar bears. This
404 number is consistent with those identified by other studies conducted in Canada (Malenfant et al.
405 2016; Jensen et al. 2020), although we did not find a unique cluster corresponding to SH
406 (Viengkone et al. 2016). The clusters we identified correspond approximately to the four polar
407 bear ecoregions that are based on life-history and sea-ice dynamics, both of which contribute to
408 genetic structure among bears (Amstrup et al. 2008). The NW subpopulation formed a unique
409 genetic cluster that is not accounted for in the ecoregions. Previous research has examined the
410 genetic structure of NW, but low samples sizes have limited the power for drawing robust

411 conclusions (Jensen et al. 2020). We found that the NW subpopulation had the greatest number
412 of private alleles despite low genetic diversity, suggesting that many of the present genetic
413 variants are unique to this subpopulation. The distinctive genetic attributes indicate that NW may
414 require special consideration when designing management plans.

415 Some caution is required when applying our results to conservation. The SNPs in our
416 analysis contained few highly differentiated loci, which contributes to the low R^2 values from the
417 models and could reduce our ability to detect variation in allele frequency that is driven by
418 natural selection. However, our primary goal was to rank the predictors of allele turnover, which
419 does not require interpreting the magnitude of the R^2 values. Additionally, climate change
420 vulnerability assessments typically require that phenotypic and genetic changes associated with
421 climate change are correlated with fitness measures (Pacifici et al. 2015; Foden et al. 2019). A
422 preliminary analysis of the lifetime reproductive success of the 50 Western Hudson Bay (WH)
423 polar bears found that individual offsets score was negatively associated with reproductive
424 success ($p = 0.08$; Figure S7). Studies that tie genome-wide measures of genetic offsets with
425 patterns of selection, gene flow, and fitness estimates are needed to fully investigate the
426 vulnerability of polar bears to climate change (Capblancq et al. 2020).

427 In this study, we have identified Canadian high Arctic polar bears as being at greater risk of
428 maladaptation to climate change. As the Arctic moves towards being ice-free in the summer,
429 polar bears must adapt quickly, disperse to lower quality habitat, or risk extirpation. Our work
430 suggests that bears that already face ice-free summers in the low and sub-Arctic are potentially
431 better suited for life in the warming Arctic. Given the extent of sea ice loss that has already
432 occurred, it is unlikely that most polar bears are adapted to current environmental conditions in
433 the Arctic. Designing conservation and management strategies for the polar bear subpopulations

434 that have the greatest capacity for adaptation may be important (Nicotra et al. 2015). However,
435 the high Arctic contains a substantial portion of standing genetic variation that is absent or rare in
436 most of the Canadian range, and conserving this unique genetic variation may improve
437 persistence across the range. Ultimately, all polar bears, and indeed all ice-adapted Arctic
438 species, are likely to face negative outcomes to climate warming. Reductions of greenhouse gas
439 emissions and protection of the remaining habitat may facilitate the long-term persistence of
440 polar bears.

441 **Statements and Declarations**

442 **Acknowledgements**

443 We would like to thank all the Inuit hunters across the circumpolar Arctic that have contributed
444 to this and other studies to further our understanding of polar bear biology. Thanks also go to R.
445 Malenfant for helpful discussion on the analysis and interpretation. Any use of trade, firm, or
446 product names is for descriptive purposes only and does not imply endorsement by the U.S.
447 Government.

448 **Funding**

449 Funding from Environment and Climate Change Canada (ECCC) provided by the Wildlife
450 Research Division and the Strategic Technology Applications of Genomics
451 in the Environment (STAGE) funding programme. Funding from the U.S. Geological Survey
452 was provided through the Ecosystems Mission Area and the Changing Arctic Ecosystems
453 Initiative. LRR was funded by and Natural Science and Engineering Research Council of Canada
454 Postdoctoral Fellowship.

455 **Conflicts of interest/Competing interests**

456 Not applicable

457 **Consent for publication**

458 All authors have read the manuscript and approve of its submission for publication.

459 **Literature Cited**

- 460 Amstrup, S., B. Marcot, and D. Douglas. 2008. A Bayesian network modeling approach to
461 forecasting the 21st century worldwide status of polar bears. In: Arctic Sea Ice Decline:
462 Observations, Projections, Mechanisms, and Implications. American Geophysical Union,
463 Washington DC.
- 464 Assis, J., L. Tyberghein, S. Bosch, H. Verbruggen, E. A. Serrão, and O. De Clerck. 2018. Bio-
465 ORACLE v2.0: Extending marine data layers for bioclimatic modelling. *Global Ecology*
466 *and Biogeography* 27:277–284.
- 467 Atwood, T. C., B. G. Marcot, D. C. Douglas, S. C. Amstrup, K. D. Rode, G. M. Durner, and J. F.
468 Bromaghin. 2016. Forecasting the relative influence of environmental and anthropogenic
469 stressors on polar bears. *Ecosphere* 7:1–22.
- 470 Barrett, R. D. H., and D. Schluter. 2008. Adaptation from standing genetic variation. *Trends in*
471 *Ecology and Evolution* 23:38–44.
- 472 Berteaux, D., D. Réale, A. G. McAdam, and S. Boutin. 2004. Keeping pace with fast climate
473 change: Can arctic life count on evolution? *Integrative and Comparative Biology* 44:140–
474 151.
- 475 Bosch, S., and S. Fernandez. 2021. sdmpredictors: Species distribution modelling predictor
476 datasets. *R package version 0.2*.
- 477 Breiman, L. 2001. Random forests. *Machine Learning* 45:5–32.
- 478 Brown, S. C., T. M. L. Wigley, B. L. Otto-Bliesner, and D. A. Fordham. 2020. StableClim,
479 continuous projections of climate stability from 21,000 BP to 2,100 CE at multiple spatial
480 scales. *Scientific Data* 7:335.
- 481 Capblancq, T., M. C. Fitzpatrick, R. A. Bay, M. Exposito-Alonso, and S. R. Keller. 2020.
482 Genomic prediction of (mal)adaptation across current and future climatic landscapes.
483 *Annual Review of Ecology, Evolution, and Systematics* 51:245–269.
- 484 Chang, C. C., C. C. Chow, L. C. A. M. Tellier, S. Vattikuti, S. M. Purcell, and J. J. Lee. 2015.
485 Second-generation PLINK: Rising to the challenge of larger and richer datasets.
486 *GigaScience* 4:1–16.
- 487 Charlesworth, B. 2009. Effective population size and patterns of molecular evolution and
488 variation. *Nature Reviews Genetics* 10:195–205.
- 489 Cohen, J., J. A. Screen, J. C. Furtado, M. Barlow, D. Whittleston, D. Coumou, J. Francis, K.
490 Dethloff, D. Entekhabi, J. Overland, and J. Jones. 2014. Recent Arctic amplification and
491 extreme mid-latitude weather. *Nature Geoscience* 7:627–637.
- 492 Comiso, J. C., C. L. Parkinson, R. Gersten, and L. Stock. 2008. Accelerated decline in the Arctic
493 sea ice cover. *Geophysical Research Letters* 35.
- 494 Docquier, D., and T. Koenigk. 2021. Observation-based selection of climate models projects
495 Arctic ice-free summers around 2035. *Communications, Earth, and Environment* 2:1–8.
- 496 Durner, G. M., and S. C. Amstrup. 1995. Movements of a polar bear from Northern Alaska to
497 Northern Greenland. *Arctic* 48:338–341.
- 498 Durner, G. M., D. C. Douglas, R. M. Nielson, S. C. Amstrup, T. L. McDonald, I. Stirling, M.
499 Mauritzen, E. W. Born, Ø. Wiig, E. Deweaver, M. C. Serreze, S. E. Belikov, M. M.
500 Holland, J. Maslanik, J. Aars, D. A. Bailey, and A. E. Derocher. 2009. Predicting 21st-
501 century polar bear habitat distribution from global climate models. *Ecological Monographs*
502 79:25–58.

503 Ellis, N., S. J. Smith, and C. R. Pitcher. 2012. Gradient forests: calculating importance gradients
504 on physical predictors. *Ecology* 93:156–168.

505 Ferguson, S. H., M. K. Taylor, E. W. Born, A. Rosing-Asvid, and F. Messier. 2002. Determinants
506 of home range size for polar bears (*Ursus maritimus*). *Ecology Letters* 2:311–318.

507 Firth, D., G. Gorjanc, S. Graves, R. Heiberger, G. Monette, H. Nilsson, D. Ogle, B. Ripley, and
508 S. Weisberg. 2009. Package ‘car.’ R Foundation for Statistical Computing.

509 Fitzpatrick, M. C., V. E. Chhatre, R. Y. Soolanayakanahally, and S. R. Keller. 2021. Experimental
510 support for genomic prediction of climate maladaptation using the machine learning
511 approach Gradient Forests. *Molecular Ecology Resources* 21:2749–2765.

512 Fitzpatrick, M. C., and S. R. Keller. 2015. Ecological genomics meets community-level
513 modelling of biodiversity: mapping the genomic landscape of current and future
514 environmental adaptation. *Ecology Letters* 18:1–16.

515 Foden, W. B., B. E. Young, H. R. Akçakaya, R. A. Garcia, A. A. Hoffmann, B. A. Stein, C. D.
516 Thomas, C. J. Wheatley, D. Bickford, J. A. Carr, D. G. Hole, T. G. Martin, M. Pacifici, J.
517 W. Pearce-Higgins, P. J. Platts, P. Visconti, J. E. M. Watson, and B. Huntley. 2019. Climate
518 change vulnerability assessment of species. *WIREs Climate Change* 10:e551.

519 Frichot, E., and O. François. 2015. LEA: An R package for landscape and ecological association
520 studies. *Methods in Ecology and Evolution* 6:925–929.

521 Frichot, E., F. Mathieu, T. Trouillon, G. Bouchard, and O. François. 2014. Fast and efficient
522 estimation of individual ancestry coefficients. *Genetics* 196:973–983.

523 Gosselin, T., Manuel Lamothe, Floriaan Devloo-Delva, and P. Grewe. 2020. radiator: RADseq
524 Data Exploration, Manipulation and Visualization using R. R package version, 1:5.

525 Gruber, B., P. J. Unmack, O. F. Berry, and A. Georges. 2018. dartr: An R package to facilitate
526 analysis of SNP data generated from reduced representation genome sequencing.
527 *Molecular Ecology Resources* 18:691–699.

528 Heemskerk, S., A. C. Johnson, D. Hedman, V. Trim, N. J. Lunn, D. McGeachy, and A. E.
529 Derocher. 2020. Temporal dynamics of human-polar bear conflicts in Churchill, Manitoba.
530 *Global Ecology and Conservation* 24:e01320.

531 Hijmans, R. J. 2023. The raster package. R package 734:473.

532 IPCC. 2023. Climate Change 2022 – Impacts, Adaptation and Vulnerability: Working Group II
533 Contribution to the Sixth Assessment Report of the Intergovernmental Panel on Climate
534 Change. Cambridge University Press, Cambridge.

535 IPCC. 2014. Climate Change 2014: Synthesis Report. Contribution of Working Groups I, II and
536 III to the Fifth Assessment Report of the Intergovernmental Panel on Climate Change.
537 Eds R.K. Pachauri and L.A. Meyer. Geneva, Switzerland.

538 IUCN/SSC Polar Bear Specialist Group. 2021. IUCN/Species Survival Commission (SSC) Polar
539 Bear Specialist Group 2021 Status Report; [https://www.iucn-pbsg.org/wp-](https://www.iucn-pbsg.org/wp-content/uploads/2021/11/July-2021-Status-Report-Web.pdf)
540 [content/uploads/2021/11/July-2021-Status-Report-Web.pdf](https://www.iucn-pbsg.org/wp-content/uploads/2021/11/July-2021-Status-Report-Web.pdf)

541 Jensen, E. L., C. Tschirter, P. V. C. de Groot, K. M. Hayward, M. Branigan, M. Dyck, R. B. G.
542 Clemente-Carvalho, and S. C. Loughheed. 2020. Canadian polar bear population structure
543 using genome-wide markers. *Ecology and Evolution* 10:3706–3714.

544 Jombart, T., and I. Ahmed. 2011. adegenet 1.3-1: New tools for the analysis of genome-wide
545 SNP data. *Bioinformatics* 27:3070–3071.

546 Jombart, T. S., S. Devillard, A.-B. Dufour, and D. Pontier. 2008. Revealing cryptic spatial
547 patterns in genetic variability by a new multivariate method. *Heredity* 101:92–103.

548 Kim, Y.-H., S.-K. Min, N. P. Gillett, D. Notz, and E. Malinina. 2023. Observationally-
549 constrained projections of an ice-free Arctic even under a low emission scenario. *Nature*
550 *Communications* 14:3139.

551 Kwok, R. 2018. Arctic sea ice thickness, volume, and multiyear ice coverage: Losses and
552 coupled variability (1958–2018). *Environmental Research Letters* 13:105005.

553 Laidre, K. L., E. W. Born, S. N. Atkinson, Ø. Wiig, L. W. Andersen, N. J. Lunn, M. Dyck, E. V.
554 Regehr, R. McGovern, and P. Heagerty. 2018. Range contraction and increasing isolation of
555 a polar bear subpopulation in an era of sea-ice loss. *Ecology and Evolution* 8:2062-2075.

556 Laidre, K. L., S. N., Atkinson, E.V., Regehr, H. L. Stern, E. Born, Ø. Wiig, N. K. Lunn, M. Dyck,
557 P. Heagerty, and B. R. Cohen. 2020. Transient benefits of climate change for a high-Arctic
558 polar bear (*Ursus maritimus*) subpopulation. *Global Change Biology* 26:6251-6265.

559 Laidre, K. L., M. A. Supple, E. W. Born, E. V. Regehr, Ø. Wiig, F. Ugarte, J. Aars, R. Dietz, C.
560 Sonne, P. Hegelund, C. Isaksen, G. B. Akse, B. Cohen, H. L. Stern, T. Moon, C. Vollmers,
561 R. Corbett-Detig, D. Paetkau, and B. Shapiro. 2022. Glacial ice supports a distinct and
562 undocumented polar bear subpopulation persisting in late 21st-century sea-ice conditions.
563 *Science* 376:1333–1338.

564 Lan, T., K. Leppälä, C. Tomlin, S. L. Talbot, G. K. Sage, S. D. Farley, R. T. Shideler, L.
565 Bachmann, Ø. Wiig, V. A. Albert, J. Salojärvi, T. Mailund, D. I. Drautz-Moses, S. C.
566 Schuster, L. Herrera-Estrella, and C. Lindqvist. 2022. Insights into bear evolution from a
567 Pleistocene polar bear genome. *Proceedings of the National Academy of Sciences*
568 119:e2200016119.

569 Láruson, Á. J., M. C. Fitzpatrick, S. R. Keller, B. C. Haller, and K. E. Lotterhos. 2022. Seeing
570 the forest for the trees: Assessing genetic offset predictions from gradient forest.
571 *Evolutionary Applications* 15:403–416.

572 Liu, S., E. D. Lorenzen, M. Fumagalli, B. Li, K. Harris, Z. Xiong, L. Zhou, T. S. Korneliussen,
573 M. Somel, C. Babbitt, G. Wray, J. Li, W. He, Z. Wang, W. Fu, X. Xiang, C. C. Morgan, A.
574 Doherty, M. J. O’Connell, J. O. McInerney, E. W. Born, L. Dalén, R. Dietz, L. Orlando, C.
575 Sonne, G. Zhang, R. Nielsen, E. Willerslev, and J. Wang. 2014. Population genomics reveal
576 recent speciation and rapid evolutionary adaptation in polar bears. *Cell* 157:785–794.

577 Lone, K., J. Aars, and R. A. Ims. 2013. Site fidelity of Svalbard polar bears revealed by mark-
578 recapture positions. *Polar Biology* 36:27–39.

579 Lotterhos, K. E., and M. C. Whitlock. 2015. The relative power of genome scans to detect local
580 adaptation depends on sampling design and statistical method. *Molecular Ecology*
581 24:1031–1046.

582 Lunn, N. J., S. Servanty, E. V. Regehr, S. J. Converse, E. Richardson, and I. Stirling. 2016.
583 Demography of an apex predator at the edge of its range – impacts of changing sea ice on
584 polar bears in Hudson Bay. *Ecological Applications* 26:1302–1320.

585 Maduna, S. N., J. Aars, I. Fløystad, C. F. C. Klütsch, E. M. L. Z. Fiskebeck, Ø. Wiig, D. Ehrich,
586 M. Andersen, L. Bachmann, A. E. Derocher, T. Nyman, H. G. Eiken, and S. B. Hagen.
587 2021. Sea ice reduction drives genetic differentiation among Barents Sea polar bears.
588 *Proceedings of the Royal Society B* 288:20211741.

589 Malenfant, R. M., D. W. Coltman, and C. S. Davis. 2015. Design of a 9K illumina BeadChip for
590 polar bears (*Ursus maritimus*) from RAD and transcriptome sequencing. *Molecular*
591 *Ecology Resources* 15:587–600.

592 Malenfant, R. M., C. S. Davis, C. I. Cullingham, and D. W. Coltman. 2016. Circumpolar genetic
593 structure and recent gene flow of polar bears: A reanalysis. *PLoS ONE* 11:1–25.

594 Malenfant, R. M., C. S. Davis, E. S. Richardson, N. J. Lunn, and D. W. Coltman. 2018.
595 Heritability of body size in the polar bears of Western Hudson Bay. *Molecular Ecology*
596 *Resources* 18:854–866.

597 Meltofte, H. 2013. Arctic Biodiversity Assessment. Status and trends in Arctic biodiversity:
598 Synthesis. Conservation of Arctic Flora and Fauna (CAFF). Arctic Council.

599 Miller, W., S. C. Schuster, A. J. Welch, A. Ratan, O. C. Bedoya-Reina, F. Zhao, H. L. Kim, R. C.
600 Burhans, D. I. Drautz, N. E. Wittekindt, L. P. Tomsho, E. Ibarra-Laclette, L. Herrera-
601 Estrella, E. Peacock, S. Farley, G. K. Sage, K. Rode, M. Obbard, R. Montiel, L. Bachmann,
602 Ó. Ingólfsson, J. Aars, T. Mailund, Ø. Wiig, S. L. Talbot, and C. Lindqvist. 2012. Polar and
603 brown bear genomes reveal ancient admixture and demographic footprints of past climate
604 change. *Proceedings of the National Academy of Sciences* 109:E2382–E2390.

605 Molnár, P. K., C. M. Bitz, M. M. Holland, J. E. Kay, S. R. Penk, and S. C. Amstrup. 2020.
606 Fasting season length sets temporal limits for global polar bear persistence. *Nature Climate*
607 *Change* 10:732–738.

608 Nei, M., and W.-H. Li. 1979. Mathematical model for studying genetic variation in terms of
609 restriction endonucleases. *Proceedings of the National Academy of Sciences of the United*
610 *States of America* 76:5269–5273.

611 Nicotra, A. B., E. A. Beever, A. L. Robertson, G. E. Hofmann, and J. O’Leary. 2015. Assessing
612 the components of adaptive capacity to improve conservation and management efforts
613 under global change. *Conservation Biology* 29:1268–1278.

614 Northrup, J.M., E. Howe, N. J. Lunn, K. Middel, M. E. Obbard, T. Ross, G. Szor, L. Walton, and
615 J. Ware. 2021. Southern Hudson Bay polar bear subpopulation aerial survey report. Final
616 report to Ontario Ministry of Natural Resources, 29 November 2021.

617 Obbard, M. E., G. W. Thiemann, E. Peacock, and T. D. DeBruyn. 2010. Polar Bears: Proceedings
618 of the 15th Working Meeting of the IUCN/SSC Polar Bear Specialist Group, Copenhagen,
619 Denmark, 29 June-3 July 2009. IUCN.

620 Oksanen, J. 2015. *Vegan: an introduction to ordination. R package version 2.6-4.*

621 Pacifici, M., W. B. Foden, P. Visconti, J. E. M. Watson, S. H. M. Butchart, K. M. Kovacs, B. R.
622 Scheffers, D. G. Hole, T. G. Martin, H. R. Akçakaya, R. T. Corlett, B. Huntley, D.
623 Bickford, J. A. Carr, A. A. Hoffmann, G. F. Midgley, P. Pearce-Kelly, R. G. Pearson, S. E.
624 Williams, S. G. Willis, B. Young, and C. Rondinini. 2015. Assessing species vulnerability
625 to climate change. *Nature Climate Change* 5:215–224.

626 Paetkau, D., Amstrup, S. C., Born, E. W., Calvert, W., Derocher, A. E., Garner, G. W., Messier,
627 F., Stirling, I., Taylor, K. M., Wigg, Ø., and Strobeck, C. 1999. Genetic structure of the
628 world’s polar bear populations. *Molecular Ecology*, 8:1571-1584.

629 Pagano, A. M., G. M. Durner, T. C. Atwood, and D. C. Douglas. 2021. Effects of sea ice decline
630 and summer land use on polar bear home range size in the Beaufort Sea. *Ecosphere*
631 12:e03768.

632 Peacock, E., A. E. Derocher, G. W. Thiemann, and I. Stirling. 2011. Conservation and
633 management of Canada’s polar bears (*Ursus maritimus*) in a changing Arctic. *Canadian*
634 *Journal of Zoology* 89:371–385.

635 Peacock, E., S. A. Sonsthagen, M. E. Obbard, A. Boltunov, E. V. Regehr, N. Ovsyanikov, J. Aars,
636 S. N. Atkinson, G. K. Sage, A. G. Hope, E. Zeyl, L. Bachmann, D. Ehrich, K. T. Scribner,
637 S. C. Amstrup, S. Belikov, E. W. Born, A. E. Derocher, I. Stirling, M. K. Taylor, Ø. Wiig,
638 D. Paetkau, and S. L. Talbot. 2015. Implications of the circumpolar genetic structure of
639 polar bears for their conservation in a rapidly warming Arctic. *PLoS ONE* 10:1–30.

640 Pembleton, L. W., N. O. I. Cogan, and J. W. Forster. 2013. StAMPP: an R package for
641 calculation of genetic differentiation and structure of mixed-ploidy level populations.
642 Molecular Ecology Resources 13:946–952.

643 Pilfold, N. W., E. S. Richardson, J. Ellis, E. Jenkins, W. B. Scandrett, A. Hernández-Ortiz, K.
644 Buhler, D. McGeachy, B. Al-Adhami, K. Konecsni, V. A. Lobanov, M. A. Owen, B.
645 Rideout, and N. J. Lunn. 2021. Long-term increases in pathogen seroprevalence in polar
646 bears (*Ursus maritimus*) influenced by climate change. Global Change Biology 27:4481–
647 4497.

648 Previdi, M., K. L. Smith, and L. M. Polvani. 2021. Arctic amplification of climate change: a
649 review of underlying mechanisms. Environmental Research Letters 16:093003.

650 R Core Team. 2023. R: A language and environment for statistical computing. R Foundation for
651 Statistical Computing, Vienna, Austria. <https://www.R-project.org/>.

652 Rantanen, M., A. Y. Karpechko, A. Lipponen, K. Nordling, O. Hyvarinen, K. Ruosteenoja, T.
653 Vihma, and A. Laaksonen. 2022. The Arctic has warmed nearly four times faster than the
654 globe since 1979. Communications Earth and Environment 3:168.

655 Regehr, E. V., N. J. Lunn, S. C. Amstrup, and I. Stirling. 2007. Effects of earlier sea ice breakup
656 on survival and population size of polar bears in western Hudson Bay. Journal of Wildlife
657 Management 71:2673–2683.

658 Regehr, E. V., K. L. Laidre, H. R. Akçakaya, S. C. Amstrup, T. C. Atwood, N. J. Lunn, M.
659 Obbard, H. Stern, G. W. Thiemann, and Ø. Wiig. 2016. Conservation status of polar bears
660 (*Ursus maritimus*) in relation to projected sea-ice declines. Biology Letters 12:20160556.

661 Rode, K. D., R. R. Wilson, E. V. Regehr, M. S. Martin, D. C. Douglas, and J. Olson. 2015.
662 Increased land use by Chukchi sea polar bears in relation to changing sea ice conditions.
663 PLoS ONE 10:1–18.

664 Romiguier, J., P. Gayral, M. Ballenghien, A. Bernard, V. Cahais, A. Chenuil, Y. Chiari, R. Dernet,
665 L. Duret, N. Faivre, E. Loire, J. M. Lourenco, B. Nabholz, C. Roux, G. Tsagkogeorga, A.-
666 T. Weber, L. A. Weinert, K. Belkhir, N. Bierne, S. Glémin, and N. Galtier. 2014.
667 Comparative population genomics in animals uncovers the determinants of genetic
668 diversity. Nature 515:261–263.

669 Screen, J. A., and I. Simmonds. 2010. The central role of diminishing sea ice in recent Arctic
670 temperature amplification. Nature 464:1334–1337

671 Shen, Z., Zhou, W., Li, J., & Chan, J. C. (2023). A frequent ice-free Arctic is likely to occur
672 before the mid-21st century. npj Climate and Atmospheric Science, 6:103.

673 Smith, T. S., Derocher, A. E., Mazur, R. L., York, G., Owen, M. A., Obbard, M. Richardson, E.
674 S., and S.C. Amstrup. 2023. Anthropogenic food: an emerging threat to polar bears. Oryx
675 57: 425-434.

676 Smith, S. J., and J. Ellis. 2013. gradientForest: Random forest functions for the census of marine
677 life synthesis project. Stern, H. L., and K. L. Laidre. 2016. Sea-ice indicators of polar bear
678 habitat. The Cryosphere 10:2027–2041.

679 Stimmelmayer, R., SimsKayotuk, C., Pederson, M., Sheffield, G., Frantz, R., Nayakik, J., Adams,
680 B. 2023. Anthropogenic waste ingestion of Southern Beaufort Sea polar bears, Alaska
681 (2010–2020). Ursus 2023:34e5.

682 Stirling, I., and W. R. Archibald. 1977. Aspects of predation of seals by polar bears. Journal of
683 Fisheries Research Board of Canada 34:1126–1129.

684 Stirling, I., and A. E. Derocher. 2012. Effects of climate warming on polar bears: A review of the
685 evidence. Global Change Biology 18:2694–2706.

686 Stroeve, J. C., T. Markus, L. Boisvert, J. Miller, and A. Barrett. 2014. Changes in Arctic melt
687 season and implications for sea ice loss. *Geophysical Research Letters* 41:6413–6419.
688 Stroeve, J., and D. Notz. 2018. Changing state of Arctic sea ice across all seasons. *Environmental*
689 *Research Letters* 13:103001.

690 Thomas, C. D., A. Cameron, R. E. Green, M. Bakkenes, L. J. Beaumont, Y. C. Collingham, B. F.
691 N. Erasmus, M. F. De Siqueira, A. Grainger, L. Hannah, L. Hughes, B. Huntley, A. S. Van
692 Jaarsveld, G. F. Midgley, L. Miles, M. A. Ortega-Huerta, A. Townsend Peterson, O. L.
693 Phillips, and S. E. Williams. 2004. Extinction risk from climate change. *Nature* 427:145–
694 148.

695 Viengkone, M., A. E. Derocher, E. S. Richardson, R. M. Malenfant, J. M. Miller, M. E. Obbard,
696 M. G. Dyck, N. J. Lunn, V. Sahanatien, and C. S. Davis. 2016. Assessing polar bear (*Ursus*
697 *maritimus*) population structure in the Hudson Bay region using SNPs. *Ecology and*
698 *Evolution* 6:8474-8484.

699 Wiig, Ø., J. Aars, and E. W. Born. 2008. Effects of climate change on polar bears. *Science*
700 *Progress* 91:151–173.

701 Wilder, J. M., D. Vongraven, T. Atwood, B. Hansen, A. Jessen, A. Kochnev, G. York, R.
702 Vallender, D. Hedman, and M. Gibbons. 2017. Polar bear attacks on humans: Implications
703 of a changing climate. *Wildlife Society Bulletin* 41:537–547.

704 Yool, A., E. E. Popova, and A. C. Coward. 2015. Future change in ocean productivity: Is the
705 Arctic the new Atlantic? *Journal of Geophysical Research: Oceans* 120:7771-7790.
706

707 **Tables and Figures**

708 Table 1. Subpopulation names, location in the high, low, and sub-Arctic, most recent abundance estimates, and year they were
 709 censused. Sample size (N) of each subpopulation included in this study is also provided, along with the primary genetic cluster
 710 assignment (see Figure 1 for visualization of cluster assignments), mean observed heterozygosity (H_o), inbreeding (F), nucleotide
 711 diversity (π), and the number of private alleles per subpopulation. Subpopulation abundance was obtained from the IUCN/SSC (2021).

Subpopulation	Location	Census Year	Abundance	N	Cluster	H_o	F	π	Private alleles
Southern Hudson Bay (SH)	sub	2016	780	37	5	0.264	0.036	0.131	469
Western Hudson Bay (WH)	low	2016	842	50	5	0.269	0.017	0.133	429
Foxe Basin (FB)	low	2010	2,585	28	5	0.269	0.016	0.133	405
Davis Strait (DS)	low	2007	2,158	32	2	0.267	0.022	0.133	295
Gulf of Boothia (GB)	low	2017	1,525	13	2	0.270	0.012	0.129	551
Baffin Bay (BB)	high	2013	2,826	28	2	0.268	0.019	0.131	336
Kane Basin (KB)	high	2014	357	10	2	0.271	0.009	0.128	667
Lancaster Sound (LS)	high	1997	2,541	30	2	0.265	0.033	0.131	315
Northern Beaufort Sea (NB)	high	2006	980	50	4	0.263	0.039	0.130	245
Southern Beaufort Sea (SB)	high	2010	900	50	4	0.259	0.054	0.130	296
M'Clintock Channel (MC)	high	2016	716	27	1	0.259	0.052	0.128	453
Viscount Melville Sound (VM)	high	1992	161	39	1	0.259	0.053	0.131	261
Norwegian Bay (NW)	high	1997	203	17	3	0.240	0.121	0.118	747

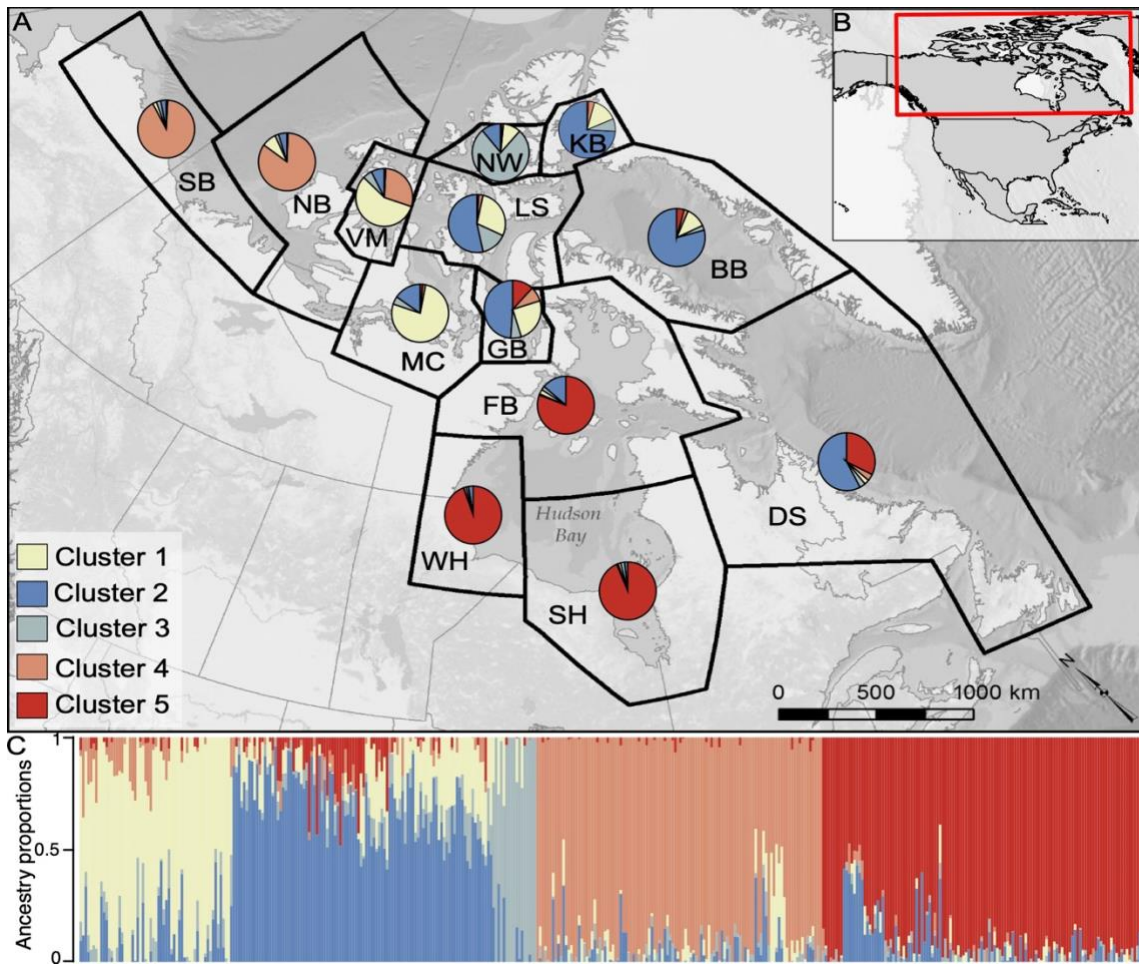


Figure 1. A) Map of ancestry coefficient proportions ($K = 5$ clusters) for each subpopulation ($N = 411$ polar bears, 3,685 SNPs). Each cluster has a subpopulation abbreviation (high Arctic: Kane Basin (KB), Lancaster Sound (LS), M'Clintock Channel (MC), Northern Beaufort Sea (NB), Norwegian Bay (NW), Southern Beaufort Sea (SB), Viscount Melville Sound (VM), Baffin Bay (BB); low Arctic: Davis Strait, (DS), Foxe Basin (FB), Gulf of Boothia (GB), Western Hudson Bay (WH); sub-Arctic: Southern Hudson Bay (SH)). Subpopulation borders recreated from Obbard et al (2022). B) Map of North America with study region highlighted in red. C) Individual ancestry proportions, where each bar represents a single individual and similar colors represent shared ancestry.

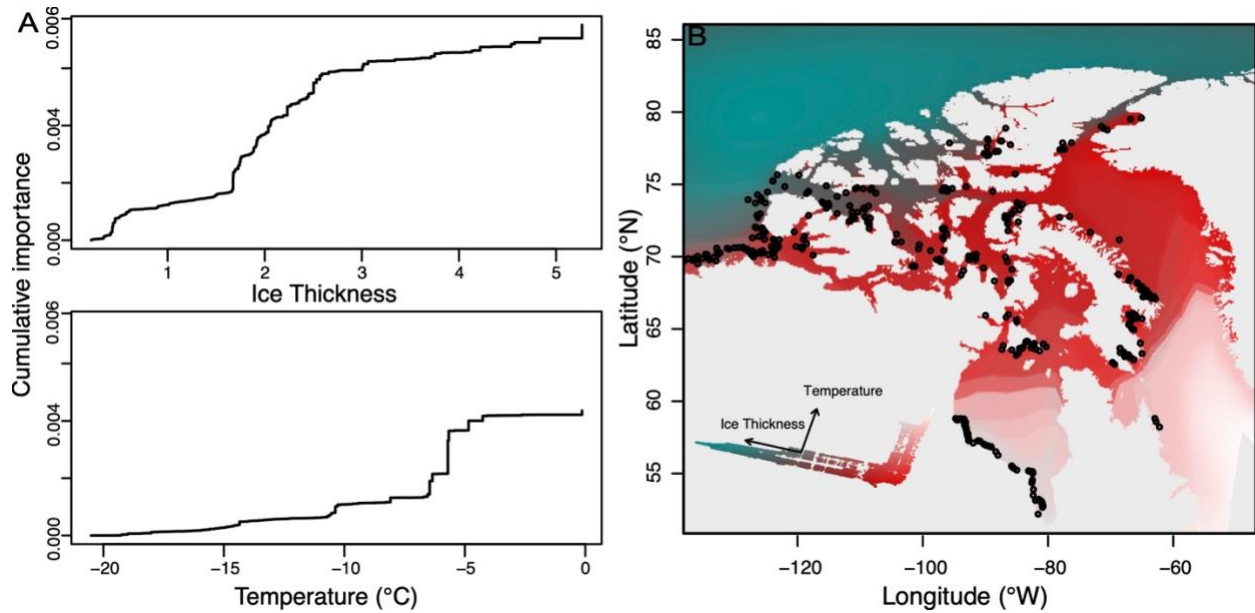


Figure 2. Allele turnover associated with ice thickness and air temperature in geographic and genetic space ($N = 411$ polar bears, 3,830 SNPs). A) Cumulative importance of allele turnover across all bears associated with the gradient in ice thickness and temperature, where steeper slopes indicate greater turnover in allele frequencies. B) Gradient in genetic turnover derived from transformed ice thickness and temperature predictors. Locations with similar colours are predicted to harbour populations with similar genetic composition. Inset depicts the PCA biplot with arrows showing the direction and magnitude of the contributions from each predictor. Points depict sampled bears.

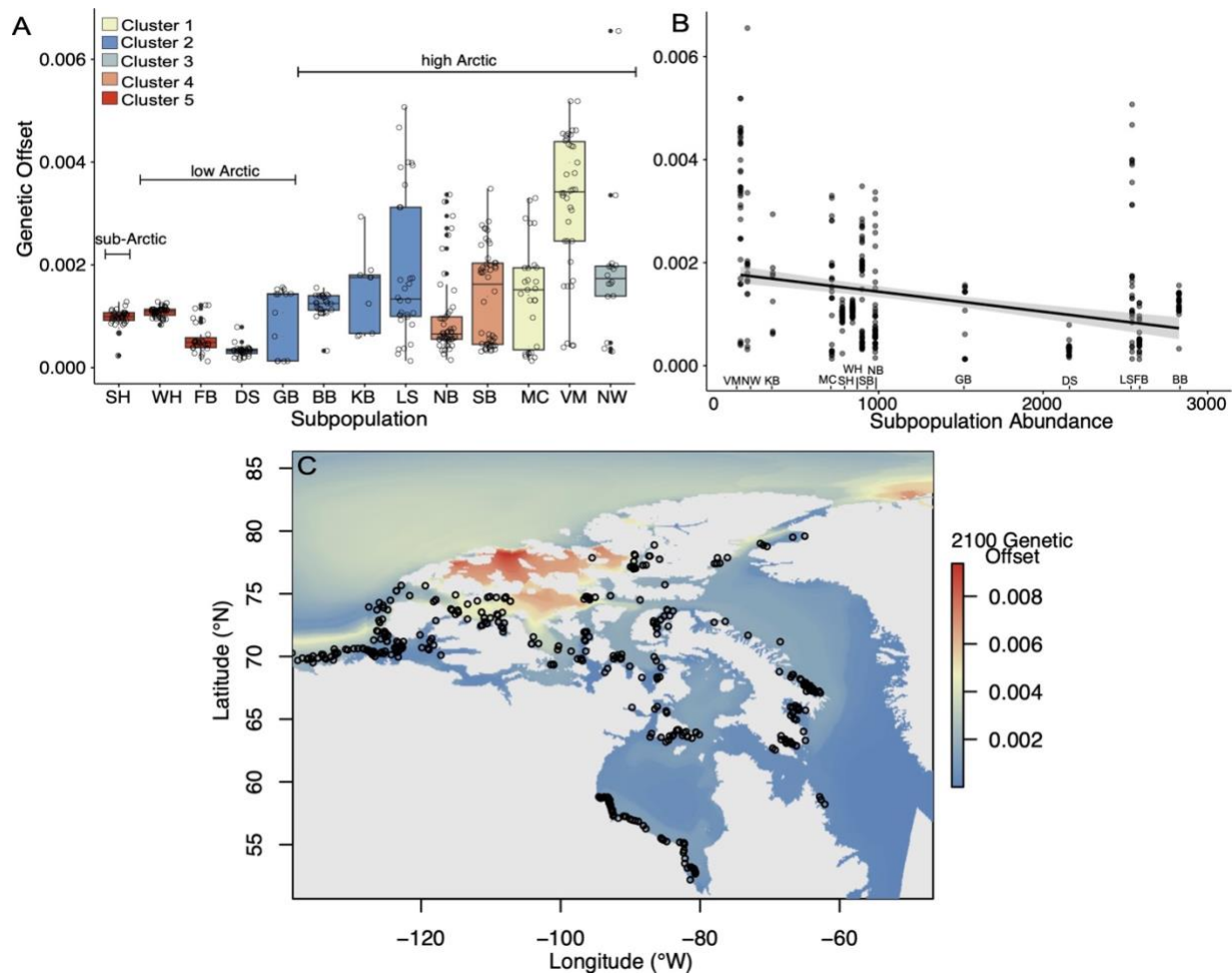


Figure 3. Genetic offset values predicted under RCP8.5 by 2100. A) Boxplot of genetic offset scores for each subpopulation, color coded by ancestry assignment (Clusters 1-5). Subpopulations are grouped into sub, low, and high Arctic categories and were significantly different from one another ($p < 0.001$). B) Genetic offsets scores as a function of subpopulation abundance. Genetic offset declined with increasing abundance ($p < 0.001$). Subpopulations are labeled on the x-axis to provide an indication of where each fall along the axis, see Table 1 for exact values. C) Individual genetic offsets ($N = 411$ polar bears, 3,830 SNPs) plotted in geographical space. Warmer colors represent higher offset, and each black point represents a polar bear individual.

Supplementary Results

Gradient Forest model of allele turnover (ice cover model)

We found a similar trend for the GF model with ice cover and temperature. Mean weighted R^2 was 0.0023. PCNM-2 was the top ranked variable ($R^2 = 0.018$). Ice cover was the second ranked variable ($R^2 = 0.015$), with the largest turnover in alleles occurring at 60% ice cover (Fig. S4a). Temperature was the fourth ranked variable ($R^2 = 0.0050$), with the largest turnover in alleles at $-5\text{ }^\circ\text{C}$ (Figure. S4a). Visualization of the PCA scores highlights a longitudinal split in genetic composition between bears that was best explained by changes in ice cover (Figure S4b). Temperature contributed to latitudinal variation in genetic composition, with Hudson Bay polar bears exhibiting stronger turnover in response to temperature than the rest of the Arctic (Figure S4b).

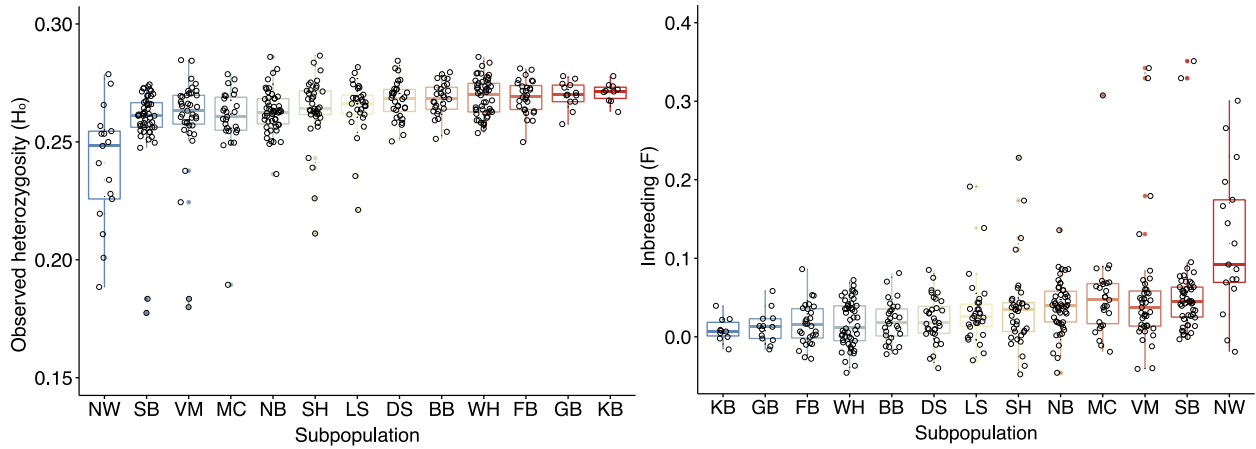
Supplemental Tables and Figures

Table S1. Mean genetic diversity for each subpopulation estimated for the complete HWE-filtered dataset ($N = 3,685$ SNPs), the RAD-derived dataset ($N = 2,304$ SNPs), and the transcriptomic-derived dataset ($N = 1,381$ SNPs).

Subpopulation	Complete		RAD-derived		Transcriptomic	
	H _o	π	H _o	π	H _o	π
Baffin Bay (BB)	0.268	0.131	0.223	0.11	0.343	0.166
Davis Strait (DS)	0.267	0.133	0.222	0.11	0.343	0.171
Foxe Basin (FB)	0.269	0.133	0.214	0.106	0.361	0.178
Gulf of Boothia (GB)	0.270	0.129	0.230	0.109	0.337	0.163
Kane Basin (KB)	0.271	0.128	0.229	0.109	0.341	0.16
Lancaster Sound (LS)	0.265	0.131	0.224	0.111	0.333	0.164
M'Clintock Channel (MC)	0.259	0.128	0.221	0.109	0.323	0.161
Northern Beaufort Sea (NB)	0.263	0.130	0.227	0.113	0.322	0.159
Norwegian Bay (NW)	0.240	0.118	0.204	0.100	0.300	0.148
Southern Beaufort Sea (SB)	0.259	0.130	0.225	0.113	0.315	0.159
Southern Hudson Bay (SH)	0.264	0.131	0.210	0.105	0.352	0.175
Viscount Melville Sound (VM)	0.259	0.131	0.223	0.112	0.320	0.161
Western Hudson Bay (WH)	0.269	0.133	0.214	0.105	0.360	0.178

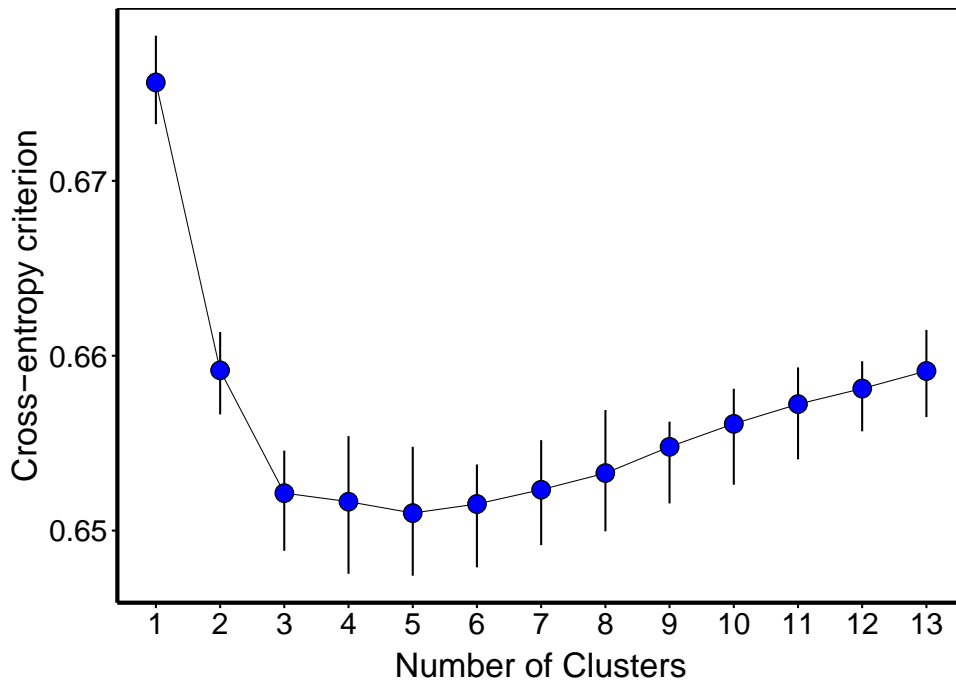
Table S2. Pairwise F_{ST} values between each subpopulation. Each pairwise comparison is significant at $p < 0.05$ except for Kane Basin-Baffin Bay ($p = 0.29$).

	BB	DS	FB	GB	KB	LS	MC	NB	NW	SB	SH	VM
Davis Strait (DS)	0.010											
Foxe Basin (FB)	0.029	0.014										
Gulf of Boothia (GB)	0.009	0.012	0.027									
Kane Basin (KB)	0.001	0.011	0.032	0.008								
Lancaster Sound (LS)	0.006	0.016	0.035	0.007	0.002							
M'Clintock Channel (MC)	0.022	0.032	0.050	0.015	0.018	0.014						
Northern Beaufort Sea (NB)	0.033	0.037	0.055	0.031	0.030	0.030	0.037					
Norwegian Bay (NW)	0.050	0.055	0.076	0.051	0.044	0.036	0.056	0.068				
Southern Beaufort Sea (SB)	0.036	0.039	0.058	0.033	0.033	0.033	0.043	0.002	0.071			
Southern Hudson Bay (SH)	0.042	0.025	0.007	0.039	0.044	0.048	0.062	0.066	0.089	0.069		
Viscount Melville Sound (VM)	0.022	0.028	0.047	0.016	0.017	0.014	0.015	0.018	0.055	0.022	0.059	
Western Hudson Bay (WH)	0.040	0.024	0.004	0.039	0.043	0.047	0.061	0.065	0.088	0.068	0.009	0.058



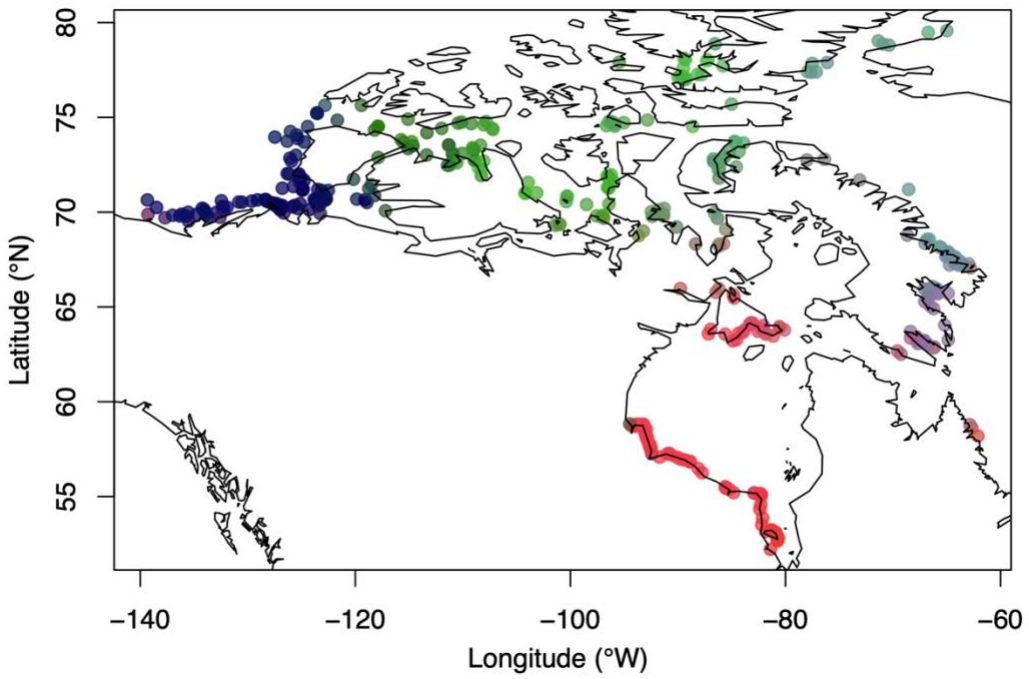
1
 2 Figure S1: Individual heterozygosity (H_o) and inbreeding (F) averaged per subpopulation.
 3 Estimated on SNPs filtered for Hardy-Weinberg Equilibrium ($N = 3,685$ SNPs).

4
 5

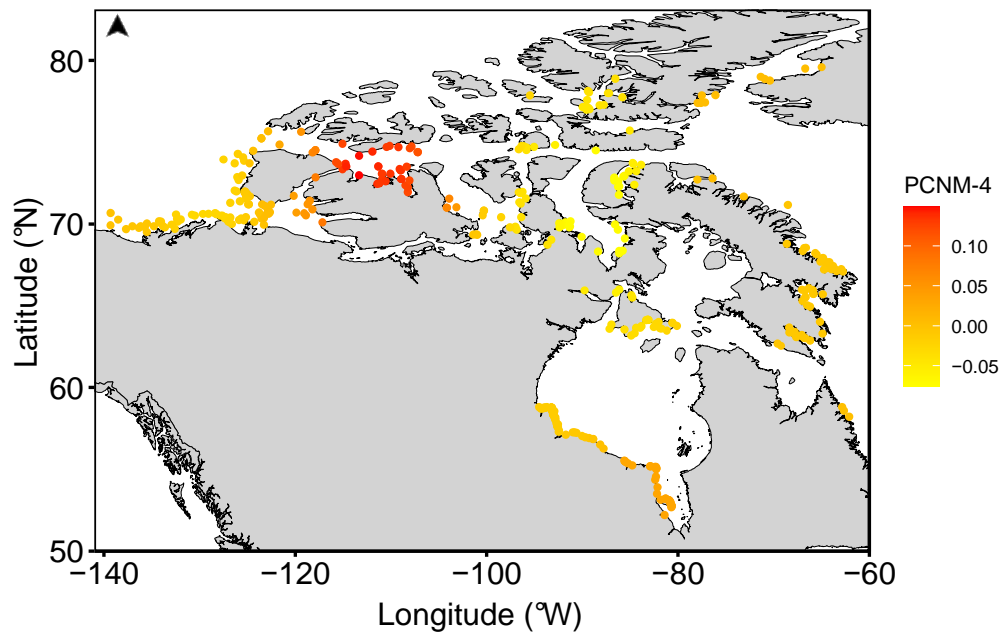
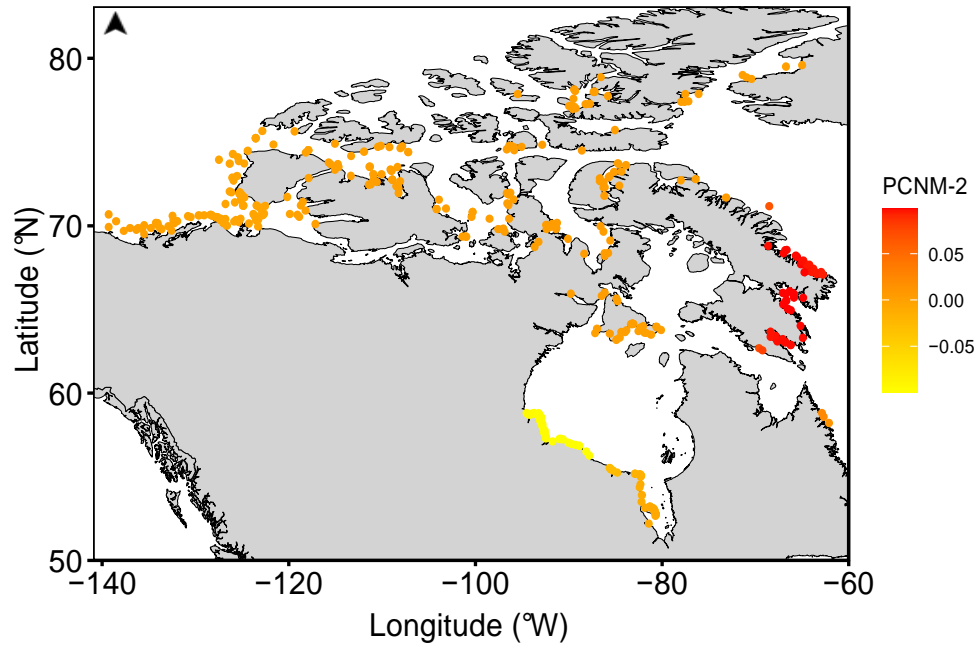


6
 7 Figure S2. Cross-entropy score comparison of clustering assignment for 411 polar bears. The
 8 model with the lowest score ($K=5$) is considered to be the best fitting model.

9

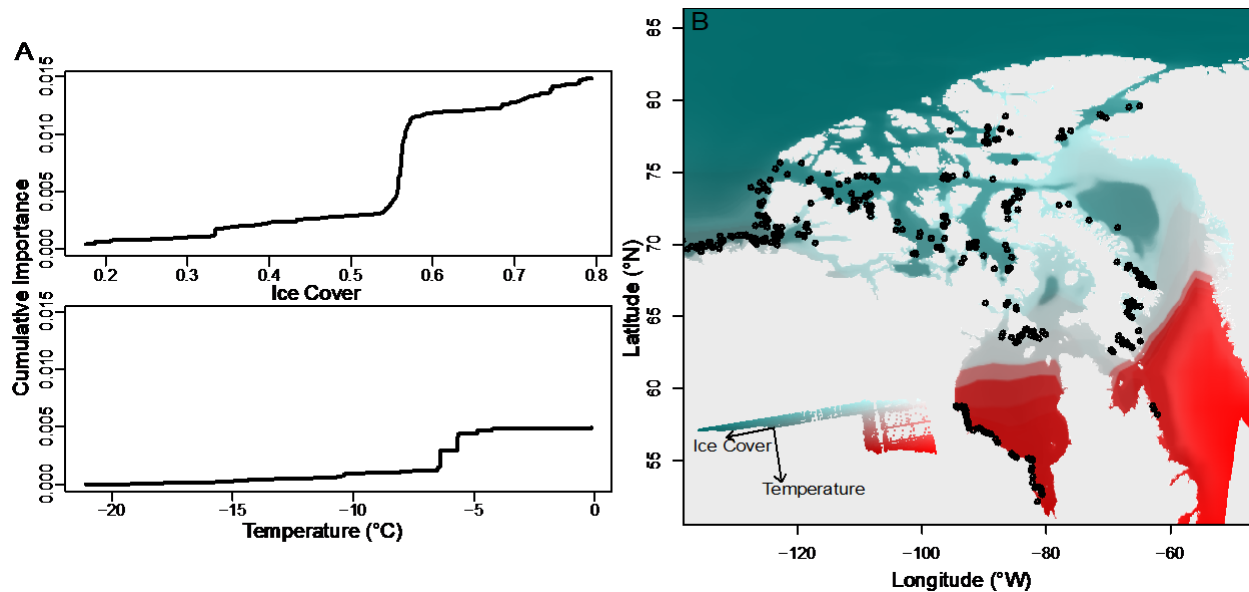


10
11 Figure S3. Translated principal component scores from the sPCA. Each point represents an
12 individual ($N = 411$, $N = 3,685$ SNPs). Similar colors indicate shared genetic variation among
13 individuals.
14
15

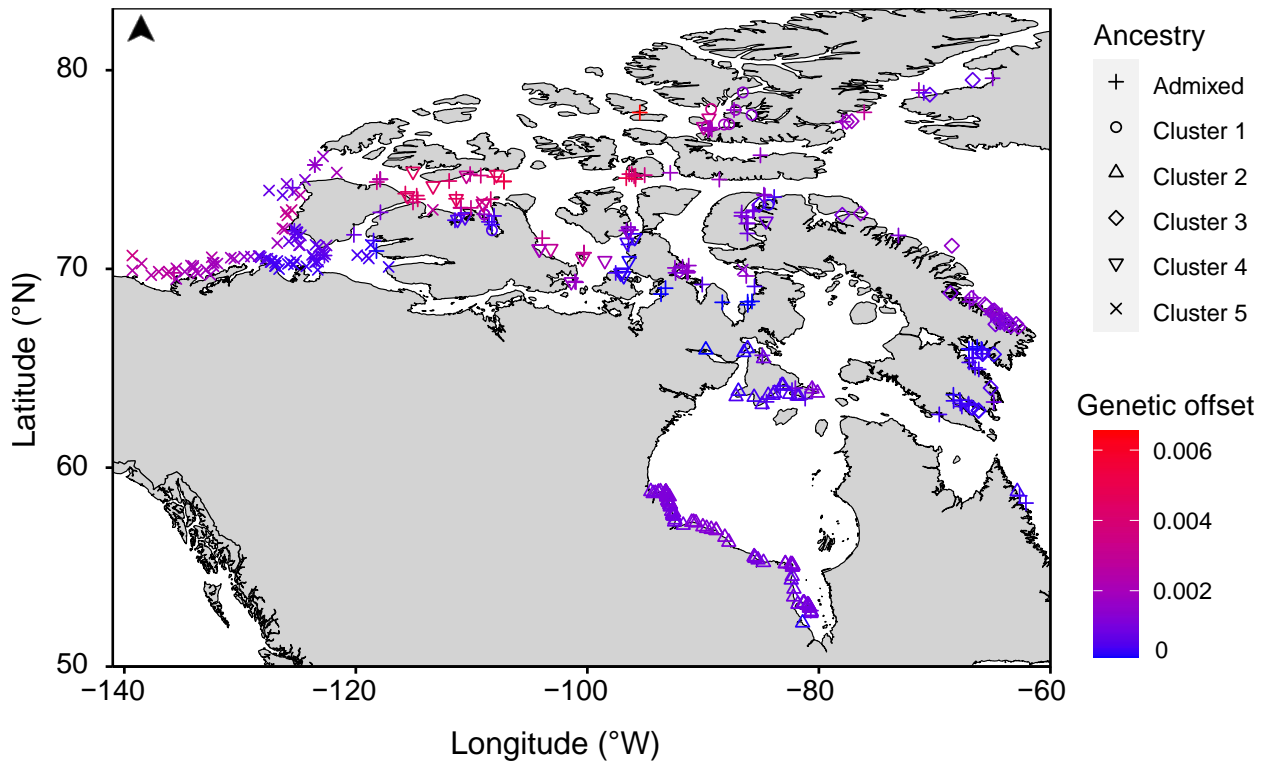


16
17
18
19
20
21
22
23

Figure S4. Map of spatial the top-ranked predictor variables from the Gradient Forest model with ice thickness and temperature. Individual sampling points are color coded by their PCNM value for each predictor. Top: Spatial scores (PCNM-2) that corresponded to variation in latitude and population abundance. Bottom: Variation in spatial scores (PCNM-4) that corresponded to maps of genetic structure among individuals.

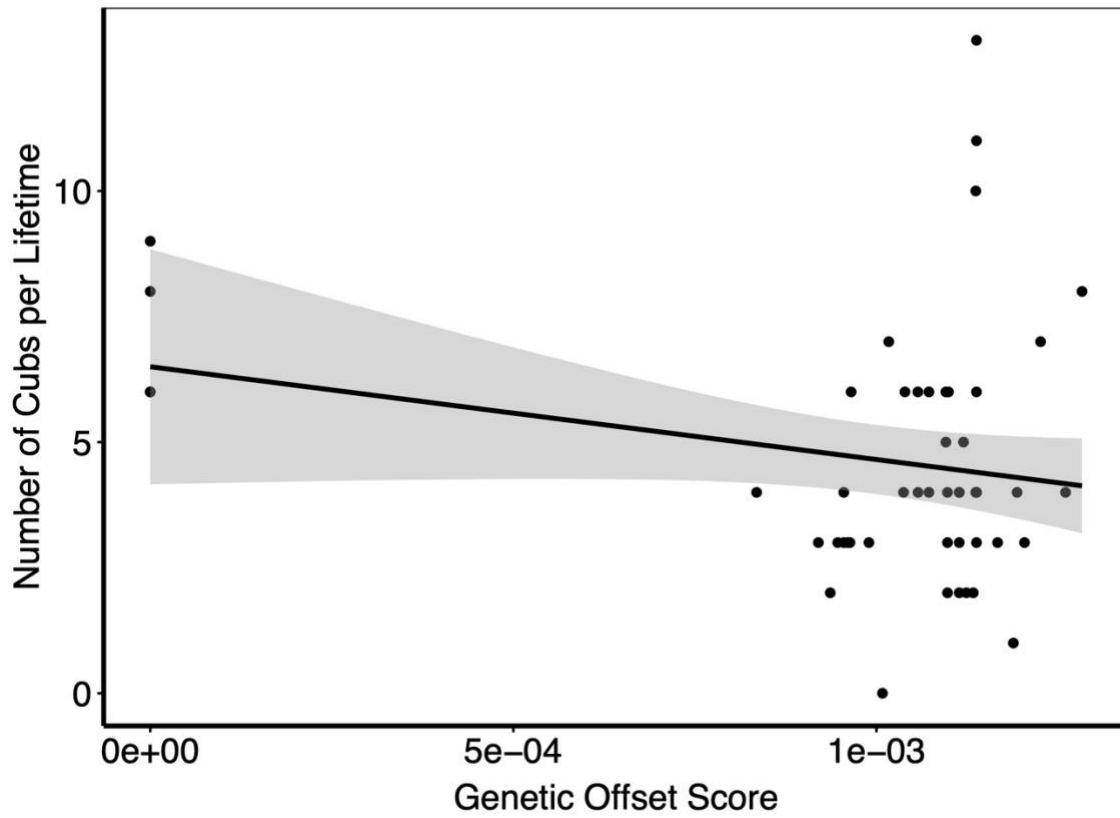


24
 25 Figure S5. Allele turnover associated with ice cover and temperature in geographic and genetic
 26 space ($N = 411$ polar bears, 3,830 SNPs). A) Cumulative importance of allele turnover across all
 27 bears associated with the gradient in ice cover and temperature, where steeper slopes indicate
 28 greater turnover in allele frequencies. B) Gradient in genetic turnover derived from transformed
 29 ice thickness and temperature predictors. Locations with similar colours are predicted to harbour
 30 populations with similar genetic composition. Inset depicts the PCA biplot with arrows showing
 31 the direction and magnitude of the contributions from each predictor. Points depict sampled
 32 bears.
 33
 34



35
36
37
38
39

Figure S6. Map of individual genetic offset scores estimated from projected environments in 2100. Color gradient denotes offset values, with blue representing low values and red representing high values. Shapes denote ancestry assignments.



40
41 Figure S7. Genetic offset scores correlated negatively ($p = 0.113$) with lifetime reproductive
42 success in 50 bears from the Western Hudson Bay subpopulation.
43
44